

Size and Cell Type Dependent Uptake of Silica Nanoparticles

I-Lun Hsiao^{1,3}, Annika Mareike Gramatke¹, Rastko Joksimovic², Marek Sokolowski², Michael Gradzielski² and Andrea Haase^{1*}

¹Federal Institute for Risk Assessment (BfR), Department Chemicals and Product Safety, Berlin, Germany

²Technische Universität Berlin, Department of Chemistry, Physical Chemistry/ Molecular Material Sciences, Berlin, Germany

³Department of Biomedical Engineering and Environmental Sciences, National Tsing Hua University, Hsinchu, Taiwan

Abstract

As silica nanoparticles (SiO₂ NP) gain increasing interest for medical applications it is important to understand their potential adverse effects for humans. Here we prepared well-defined core-shell fluorescently labelled SiO₂ NP of 15, 60 and 200 nm diameter and analyzed their cytotoxicity in THP-1 derived macrophages, A549 epithelial cells, HaCaT keratinocytes and NRK-52E kidney cells. We observed a size-dependent cytotoxicity in all cell types in serum-free conditions. HaCaT cells were least and macrophages or lung derived A549 cells were highly sensitive towards SiO₂ NP treatment. Differences in cytotoxicity could be correlated with different uptake rates. By using flow cytometry and confocal microscopy we quantified the uptake. Furthermore we used specific inhibitors for clathrin- and caveolin-mediated endocytosis to elucidate the uptake mechanisms, which were found to be dependent on the NP size and the cell type. Clathrin-mediated endocytosis was involved in the uptake of SiO₂ NP of all sizes and was the major pathway for 60 nm or 200 nm SiO₂ NP. Caveolin-mediated endocytosis contributed to the uptake of 60 and 200 nm SiO₂ NP in THP-1 macrophages but only to uptake of 200 nm SiO₂ NP in A549. However, in the presence of serum all SiO₂ NP were non-toxic. The presence of serum furthermore could alter the uptake mechanism. In summary, this study demonstrates size- and cell type dependent differences in SiO₂ NP uptake and toxicity.

Keywords: Silica nanoparticles; Core-shell nanoparticles; Uptake mechanisms; Endocytosis; Cytotoxicity

Abbreviations: AAS: Atomic Absorption Spectroscopy, APTS: (3-Aminopropyl)-triethoxysilane, CLSM: Confocal Laser Scanning Microscopy, CME: Clathrin-mediated Endocytosis, DLS: Dynamic Light Scattering, DMEM: Dulbecco's Modified Eagle's Medium, DMSO: Dimethyl Sulfoxide, FACS: Flow Cytometry; FCS: Foetal Calf Serum, HBSS: Hank's Balanced Salt Solution; ICP-MS: Inductively Coupled Plasma Mass Spectrometry; ICP-OES: Inductively Coupled Plasma Optical Emission Spectrometry; LacCer: Lactosylceramide; NM: Nanomaterials; NP: Nanoparticles; NRK: Normal Rat Kidney; PBS: Phosphate Buffered Saline; PFA: Paraformaldehyde; PMA: phorbol-12-myristate-13-acetate; ROS: Reactive Oxygen Species; SiO₂ NP: Silica Nanoparticles; TEOS: Tetraethoxysilane; TEM: Transmission Electron Microscopy

Introduction

Nanomaterials (NM) are gaining increasing interest for various fields of application. They are used in the medical sector, in consumer products, for building materials, in computer technology or for waste remediation. By yearly production volumes and by number of products, silica nanoparticles (SiO₂ NP) belong to the highest commercialized NP, ranked as number 4 by the project of emerging nanotechnology [1]. SiO₂ NP are frequently used in consumer products and in nanocomposites, where they can act as a binder in ceramics or increase the scratching resistance of varnishes [1-3]. Furthermore, they gained huge interest in medicine for gene or drug delivery, in cancer therapy and for imaging purposes [4]. SiO₂ are very versatile NP. They can be easily synthesized in various well defined sizes and can be easily surface modified. Thus, they can be labeled with different dyes for imaging purposes or with antibodies for specific targeting [5,6]. Mesoporous variants can be loaded with drugs. Due to their increasing use and the various interesting possible future applications it is important to analyze putative hazards of SiO₂ NP for humans.

In principle several uptake routes need to be considered, i.e. dermal, intestinal, inhalative or for medical applications also intravenous injections. It is known that after systemic uptake, NP can

be transported to secondary organs such as kidney, liver, spleen and eventually also to the brain [7]. In short term inhalation studies non-surface modified amorphous SiO₂ was able to induce slight or marked inflammation [8,9]. Pulmonary inflammation and lung tissue damage was also detected in instillation studies in mice [10]. Skin penetration of SiO₂ NP was detected *in vivo* and *in vitro* [11,12]. After three days of topical exposure to the ear skin in mice SiO₂ NP were detected inside Langerhans cells and in the cervical lymph nodes [11]. In human skin explants they could be detected in epidermal and dendritic cells [12]. In an oral study elevated silica levels were found in the spleen after 84d in the highest dose group [13]. After iv injection SiO₂ NP were found in the muscle, bone, skin, liver, lung and spleen [14,15] with detectable changes in histopathology for liver, spleen and lung tissues [15].

Toxicity of SiO₂ NP was studied in different cell types. SiO₂ NP may induce cytotoxicity or apoptosis and lead to inflammation, DNA damage, or lipid peroxidation in various cell lines [16-20]. These adverse effects could be mediated by oxidative stress or/and the activation of stress-related signalling pathways [21,22]. The toxicity appears to be dependent on NP size and surface [17,23-26]. For instance, Li et al. have demonstrated that SiO₂ NP with diameters of 19, 43, 68 and 498 nm cause cytotoxicity, increased reactive oxygen species (ROS) level, DNA damage and cell cycle arrest in HepG2 cells in a size-dependent manner [23]. Other studies also detected size-dependent inflammation [25,26]. Furthermore toxicity seems to be dependent on the cell line [27,28]. For instance, skin derived HaCaT cells appeared to be more resistant towards 14 nm SiO₂ NP compared to lung derived A549 and

*Corresponding author: Andrea Haase, Max-Dohm-Str. 8-10, D - 10589 Berlin, Germany, Tel: 49-30-18412-3423; Fax: 49-30-6-18412-3423; E-mail: andrea.haase@bf.bund.de

Received November 05, 2014; Accepted November 24, 2014; Published December 03, 2014

Citation: Hsiao I, Gramatke AM, Joksimovic R, Sokolowski M, Gradzielski M, et al. (2014) Size and Cell Type Dependent Uptake of Silica Nanoparticles. J Nanomed Nanotechnol 5: 248. doi: [10.4172/2157-7439.1000248](https://doi.org/10.4172/2157-7439.1000248)

Copyright: © 2014 Hsiao I, et al. This is an open-access article distributed under the terms of the Creative Commons Attribution License, which permits unrestricted use, distribution, and reproduction in any medium, provided the original author and source are credited.

HT29 colon cells [29]. Different forms of SiO₂ NP, ie mesoporous, crystalline, or amorphous also show differences in toxicity [30-32]. Crystalline SiO₂ induced sustained pulmonary inflammation in *in vivo* instillation, while the responses to amorphous SiO₂ NP were reversible [33]. Intraperitoneal application of mesoporous but not of amorphous colloid silica SiO₂ led to systemic immune responses in mice [34]. Taken together there is various evidence, that SiO₂ NP may be taken up through various routes, reach secondary target organs and may also lead to adverse effects. The uptake and the toxicity mechanisms are not understood in detail. However, in particular for medical applications it is important to understand and to control the uptake of the NP as this may critically affect the drug efficiency.

For this purpose the uptake into various cells and tissues needs to be quantified. This may be done via inductively coupled plasma mass spectrometry (ICP-MS), optical emission spectroscopy (ICP-OES), or atomic absorption spectroscopy (AAS) [35-38]. However, none of these methods is able to determine NP localization. For this purpose many studies use fluorescently labeled SiO₂ NP [22,25,27,28,39-43]. By combining flow cytometry and confocal microscopy it is possible to get time and space resolved semi-quantitative and qualitative uptake information [42]. Furthermore, it is feasible to perform quantification in flow cytometry after determining average fluorescent intensity per particle. A size-, time- and cell type-dependent uptake has been shown for fluorescent-labeled SiO₂ NP in several studies [22,27,40,42,43]. Uptake mechanisms are less well analyzed. It is known that endocytosis is involved in uptake of SiO₂ NP in HepG2 [40], THP-1 [22], A549 [22,42], HeLa [43], and NCI-H292 cells [44]. Smaller SiO₂ NP may also translocate in cells via energy independent pathways or even by passive diffusion [28,43,44]. Endocytosis can be differentiated into clathrin-mediated or caveolin-mediated endocytosis. Clathrin-mediated endocytosis seems to mediate uptake of a wide size range of particles (55.6 nm ~ 600 nm) in different cell types [17,27,40,43], while size range for caveolin-mediated endocytosis is much more limited [17,43]. In addition there are also clathrin- and caveolin-independent uptake pathways [25,41].

NP are altered in biological media for instance by the formation of a so-called protein corona. This will influence the NP uptake and the uptake mechanisms. In the presence of serum SiO₂ NP show a reduced adhesion to cell membrane and a reduced uptake [45,46]. Formation of a corona can also increase NP agglomeration [47,48]. Recently, there are indications that uptake mechanisms are altered in the presence or absence of a protein corona [49,50].

Unfortunately, nearly all these studies suffer from major drawbacks. Dye-labeled SiO₂ NP may release a certain amount of dye over time by so-called dye leakage [51]. Usually the dye is attached to the surface, which can alter the surface properties and may have a strong influence on the uptake mechanisms on its own [27]. Thus, our motivation was to apply core-shell fluorescently labeled SiO₂ NP, which are protected by an additional silica shell. We used three different sizes of this core-shell SiO₂ particles (diameters of 15, 60 and 200 nm). We analyzed size dependent uptake and uptake mechanisms in four different relevant cell lines representing different uptake routes. Human lung adenocarcinoma epithelial cell line (A549) were used as a lung related cell line and human keratinocyte cell line (HaCaT) as a skin related cell line. THP-1 derived macrophages and rat kidney epithelioid cell line (NRK-52E) are models for important secondary targets. We studied the uptake by flow cytometry and confocal microscopy and used different inhibitors to get insights into the uptake mechanisms. Studies were performed in the presence and absence of serum.

Materials and Methods

Synthesis of nanoparticles

Dye-labeled SiO₂ NP with silica coating were prepared in three steps: synthesis of SiO₂ NP, labeling with dye and final silica coating. The 60 and 200 nm SiO₂ NP were synthesized as published [52], while 15 nm particles were from a commercial source (Ludox SM, obtained as a 30% wt. suspension in H₂O, Sigma-Aldrich, Taufkirchen, Germany). The surface was functionalized with (3-Aminopropyl)-triethoxysilane (APTS, ≥ 98%, Sigma-Aldrich, Taufkirchen, Germany). For labeling Alexa Fluor 488 5-SDP Ester (Invitrogen, Darmstadt, Germany) was dissolved in ethanol (1.5×10⁻⁴ g^{Alexa} / g^{Ethanol}), added to the suspension of aminated SiO₂ NP, which has been adjusted to pH 5 and left stirring overnight. Alexa-labeled SiO₂ dispersions were then adjusted to a pH of 8-9 before adding lysine and sonicated for 2 h. As a catalyst for the formation of the silica shell 35-45 mg of lysine was added, followed by dropwise addition of 0.08-0.17 g tetraethoxysilane (TEOS, ≥ 98%, ABCR, Germany) at 60°C and reacted overnight. After coating the SiO₂ dispersions were dialyzed in water. We confirmed an approximately 1.5 nm thick layer around the Alexa-labeled SiO₂ NP by dynamic light scattering (DLS) and transmission electron microscopy TEM (Figure S1). Two batches of submicron silica particles were synthesized, both approximately 200 nm. One (221 nm) was used in toxicity and uptake studies, and another one (177 nm) was used to study uptake mechanisms. For both batches cytotoxicity and quantification of uptake by flow cytometry has been analyzed.

NP were stable for several month and no dye leakage was detected for up to 6 month (Figure S2). For this purpose NP were depleted by ultracentrifugation and the supernatants have been analysed by fluorescence spectrometry (Perkin Elmer, Rodgau, Germany). For control purposes the NP suspensions as well as pure water has been analysed.

Suspension of nanoparticles

Suspensions of particles were freshly prepared before each experiment. Stock solutions of SiO₂ NP were first ultrasonicated in an ultrasonication bath (Sonorex, Bandelin, Berlin, Germany) for 5 min while cooled in an ice bath and then diluted to 2.5 mg/mL in the indicated medium and stirred at 700 rpm for 1 h at room temperature to achieve optimal dispersion.

Characterization of nanoparticles

Primary sizes and morphology of SiO₂ NP were measured by transmission electron microscope (TEM, Tecnai G² 20 S-TWIN, FEI, Oregon, USA) as published elsewhere [52]. The hydrodynamic diameters of SiO₂ NP were examined by dynamic light scattering (DLS) (Zetasizer Nano ZS, Malvern, Herrenberg, Germany) at room temperature. Particles were diluted for DLS measurement to a final concentration of 100 µg/mL.

Cell culture

THP-1 cells (ACC 16 from DSMZ, Braunschweig, Germany) were cultured in RPMI 1640 medium supplemented with 10% foetal calf serum (FCS), 1% L-glutamine, 1% penicillin/streptomycin, 1% Hepes and 1% sodium pyruvate. A549 cells (obtained via EU FP7 QualityNano project from UCD, Dublin, Ireland) were cultured in Ham's F12 medium supplemented with 10% FCS, 1% L-glutamine and 1% penicillin/streptomycin. HaCaT cells (CLS Cell Lines Service GmbH, Eppelheim, Germany) were cultured in DMEM medium supplemented with 10% FCS, 1% L-glutamine and 1% penicillin/

streptomycin. NRK-52E cells (ACC 199, DSMZ, Braunschweig, Germany) were cultured in Dulbecco's Modified Eagle's high glucose medium (DMEM) supplemented with 10% FCS, 1% L-glutamine, 1% penicillin/streptomycin and 2.5% HEPES. All cell lines were cultivated at 37°C, 5% CO₂ and with 95% relative humidity. Phorbol-12-myristate-13-acetate (PMA) at 100 ng/mL for 24h was used to differentiate THP-1 cells into macrophages like cells.

Cytotoxicity

WST-1 cell viability assay was used to evaluate the toxicity of SiO₂ NP according to manufacturer instructions (Roche Diagnostics, Mannheim, Germany). Cells were treated 24 h after seeding in 96-well plates with 10, 20 and 50 µg/mL SiO₂ NP for 24 h. As positive control, dimethyl sulfoxide (DMSO) was used (10 µL for THP-1, A549 and NRK-52E cells, 20 µL for HaCaT cells). Interfering NP were removed in a table top centrifuge by centrifugation with maximum speed prior to spectrophotometric read-out (TECAN, Switzerland) at 450 nm. Mean values ± SEM are given from three independent experiments.

Confocal microscopy

Cells were treated with SiO₂ NP suspensions at 20 µg/mL 24 h after seeding (2.5×10⁵ cells/mL) on coverslips in 6-well culture plates. After 2 or 24 h of incubation, cell nuclei were stained by Hoechst 33342 (Life Technologies, Darmstadt, Germany) (100 ng/mL, 5 min). 50 nM LysoTracker Red (Life Technologies, Darmstadt, Germany) were added 30 min before end of treatment. Cells were washed three times with phosphate buffered saline (PBS) and were fixed with 4% paraformaldehyde (PFA) in PBS (pH 7.4). Images were obtained by confocal laser scanning microscopy (CLSM) system LSM 700 (Carl Zeiss, Göttingen, Germany) with a 63 × oil-immersion objective using 488 nm laser for Alexa-488, 405 nm for Hoechst33342 and 555 nm for LysoTracker Red.

Immunofluorescence

Cells were seeded as for CLSM analysis. As positive substrates we used BODIPY-LacCer (1 µM, Life Technologies, Darmstadt, Germany) for Caveolin mediated or FITC-Transferrin (10 µg/mL, Life Technologies, Darmstadt, Germany) for Clathrin mediated endocytosis in serum-free medium for 1.5 h. Cells were washed three times with PBS and were fixed with 4% PFA. For immunofluorescence cells were stained as described elsewhere [53]. Primary antibodies (anti-caveolin or anti-clathrin, New England Biolabs, Frankfurt a.M., Germany) were diluted in HBSS (Hank's balanced salt solution) at 1:200 and applied overnight at 4°C. Secondary antibody (Alexa-546 goat-anti-rabbit, Life Technologies, Darmstadt, Germany) was diluted 1:200 and applied for 1.5 h at room temperature. Cells were mounted using Vectashield mounting medium (Linaris GmbH, Dossenheim, Germany).

Flow Cytometric analysis (FACS)

For FACS analysis 2.5×10⁵ cells/mL were seeded into 6-well plates for 24h, then medium was replaced to serum-free medium (if indicated). Cells were exposed to 10, 20 and 50 µg/mL SiO₂ NPs for 2 or 24 h, were washed three times with PBS, detached by 0.05% trypsin/EDTA (A549, HaCaT and NRK-52E cells) or accutase (THP-1 macrophages), harvested by centrifugation, washed again with PBS and resuspended in PBS for FACS analysis. The fluorescence of 20,000 cells was detected at FITC channel after excitation at 488 nm laser using a BD FACSAriaIII (BD biosciences, Heidelberg, Germany).

For studying uptake mechanisms A549 and THP-1 cells were pre-treated for 30 min with 50 or 100 µM genistein (24h or 2 h, respectively),

1 or 2.5 µg/mL filipin III (24h or 2 h, respectively), and 5 µg/mL chlorpromazine hydrochloride (all from Sigma-Aldrich, Munich, Germany). For potassium-depletion, cells were washed with PBS, with potassium-depletion buffer (20 mM HEPES pH 7.4, 140 mM NaCl, 1 mM CaCl₂, 1 mM MgCl₂, 1 mg/mL D-glucose) and then incubated in hypotonic buffer (1:1 ratio of potassium-depletion buffer and H₂O) for 10 min at 37°C before being transferred to potassium-depletion buffer for 30 min. Controls were untreated cells (for genistein, filipin or chlorpromazine) or cells treated by potassium-depletion buffer supplemented with 10 mM KCl. For inhibitor studies SiO₂ NP were used at 10 µg/mL for 2 and 24 h of exposure. External fluorescence was quenched using 0.1% Trypan blue. Uptake was quantified by FACS analysis. BODIPY-LacCer (lactosylceramide complexed to BSA, 0.5 µM) and transferrin-fluorescein conjugate (10 µg/mL) were used as control substrates.

Statistics

All experiments are performed in three independent repeats. Data were presented as means ± SEM. Analysis was done using GraphPad Prism 5.0.

Results

Characterization of SiO₂ NP

The SiO₂ NP used in this study contained a silica core, which was labeled with the fluorescent dye Alexa Fluor 488 and then further covered by another silica layer (Figure 1A). NP suspensions were analyzed by dynamic light scattering (DLS) prior to use in water or cell culture medium (Figure 1B and Table 1). TEM was used to confirm shape and size (Figures 1C to 1E). All particles were spherical and uniform in size. Sizes and zeta potentials are listed in Table 1.

In general, our NP were very well dispersed in water and in serum-free cell culture medium. Only the 15 nm SiO₂ NP showed some agglomeration, which can be attributed to the relatively larger surface area and the thereby increased attractive van der Waals interactions. In the presence of serum the 15 and 60 nm SiO₂ NP form agglomerates. The zeta potentials were very similar for all NP.

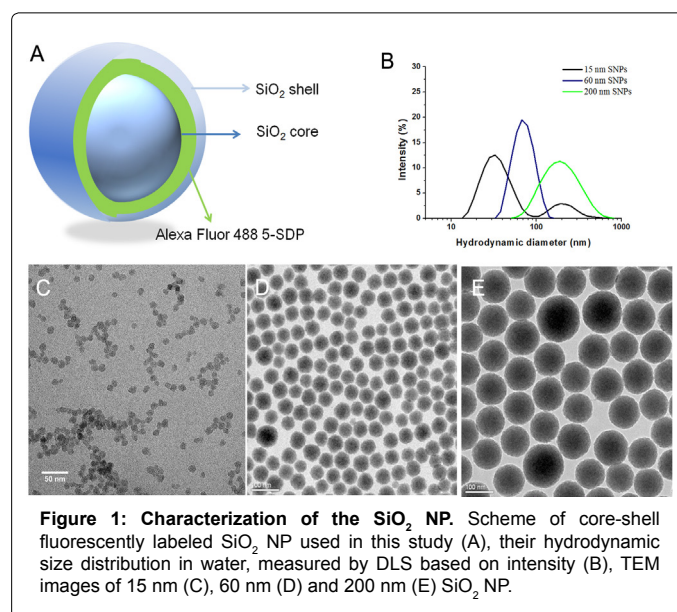


Figure 1: Characterization of the SiO₂ NP. Scheme of core-shell fluorescently labeled SiO₂ NP used in this study (A), their hydrodynamic size distribution in water, measured by DLS based on intensity (B), TEM images of 15 nm (C), 60 nm (D) and 200 nm (E) SiO₂ NP.

SiO ₂ NP	Hydrodynamic diameter (nm) ^b				Polydispersity index (Pdl)			Zeta (mV)
	water	RPMI ^c	RPMI ^c 24h	RPMI (10% FCS)	water	RPMI ^c	RPMI (10% FCS)	water
15 nm	42.7±0.9	41.3±1.3	226.9±3.4	70.8±0.3	0.40±0.03	0.39±0.03	0.61±0.01	-28.1±0.7
60 nm	67.9±0.7	68.8±1.0	325.2±6.6	158.2±3.0	0.05±0.01	0.05±0.01	0.48±0.01	-30.6±1.2
200 nm	176.5±3	124.0±2	276.5±3.0	148.1±2.5	0.19±0.02	0.02±0.01	0.34±0.03	-31.8±1.6

^aAll measurement were performed at 25 °C at 100 µg/mL.

^bHydrodynamic diameter was determined as Z-average (% intensity), which was derived from the cumulant mean of the intensity autocorrelation function.

^cThe hydrodynamic diameters were measured in serum-free RPMI medium.

Table 1: Physicochemical characterization of SiO₂ NP^a.

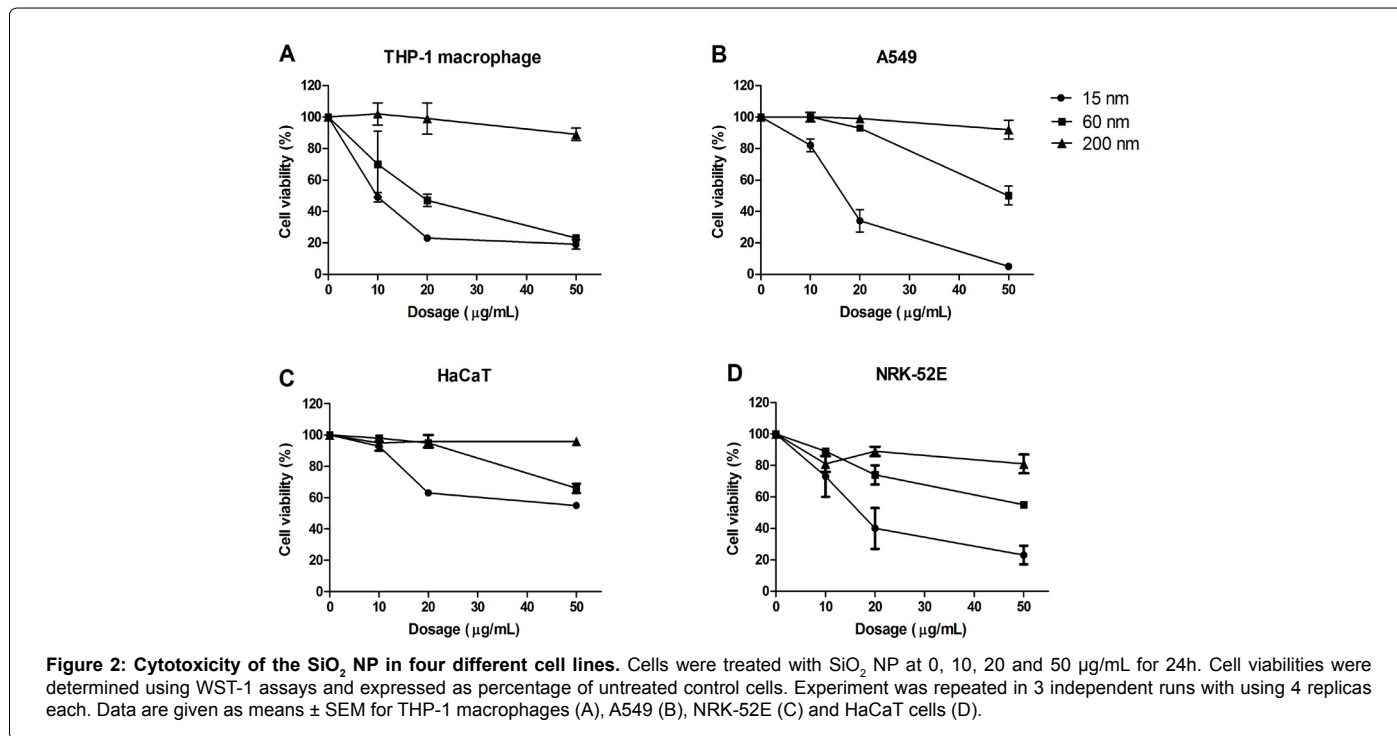


Figure 2: Cytotoxicity of the SiO₂ NP in four different cell lines. Cells were treated with SiO₂ NP at 0, 10, 20 and 50 µg/mL for 24h. Cell viabilities were determined using WST-1 assays and expressed as percentage of untreated control cells. Experiment was repeated in 3 independent runs with using 4 replicas each. Data are given as means ± SEM for THP-1 macrophages (A), A549 (B), NRK-52E (C) and HaCaT cells (D).

SiO ₂ NPs	THP-1 macrophage	A549	HaCaT	NRK-52E
15 nm	10	15	-	15
60 nm	18	50	-	-
200 nm	-	-	-	-

^a indicates that the IC₅₀ could not be determined as cell viability did not decline to 50%.

Table 2: IC₅₀ (µg/mL) of SiO₂ NP after 24 h of treatment with four cell lines.

Because of the strong agglomeration of our SiO₂ NP in serum-containing medium, the main part of this study was done in serum-free medium, i.e prior to NP exposure cells were set to serum-free medium. However, we also included analysis of NP uptake in serum containing cell culture medium and compared this to serum-free conditions.

SiO₂ NP cytotoxicity is dependent on size and on cell type

Cells were exposed to SiO₂ NP at concentrations of 10, 20 and 50 µg/mL for 24 h and the cell viability was determined using WST-1 assay. Data are shown in Figure 2 and summarized in Table 2. The 15 nm SiO₂ NP caused significant cytotoxicity to all tested cell lines. The 60 nm SiO₂ NP caused less pronounced cytotoxicity, if applied doses were compared on mass basis. The 200 nm particles did not display any cytotoxicity in all four cell lines at all applied doses. Most prominent effects towards all NP were observed for THP-1 macrophages (Figure 2A and Table 2), which had an IC₅₀ value of 10 and 18 µg/mL for the 15 nm and 60 nm

SiO₂, respectively. Also in A549 cells (Figure 2B) significant effects were observed, with IC₅₀ values of 15 and 50 µg/mL for 15 nm and 60 nm NP, respectively. HaCaT cells were rather insensitive, and an IC₅₀ could not be reached for any size of SiO₂ NP (Figure 2C). NRK-52E cells showed pronounced effects only towards the 15 nm SiO₂, the IC₅₀ value was 15 µg/mL (Figure 2D). Interestingly, in serum-containing media no cytotoxicity was observed for all sizes of particles.

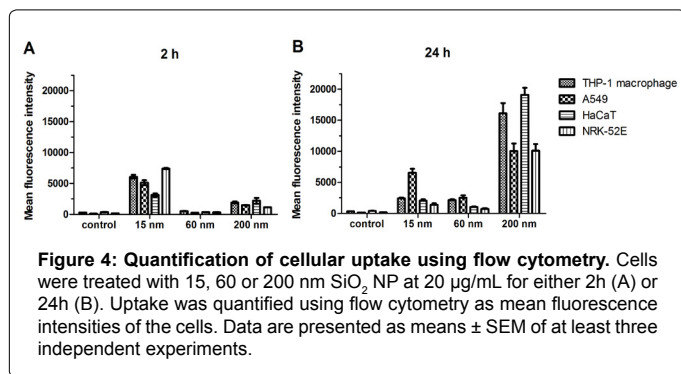
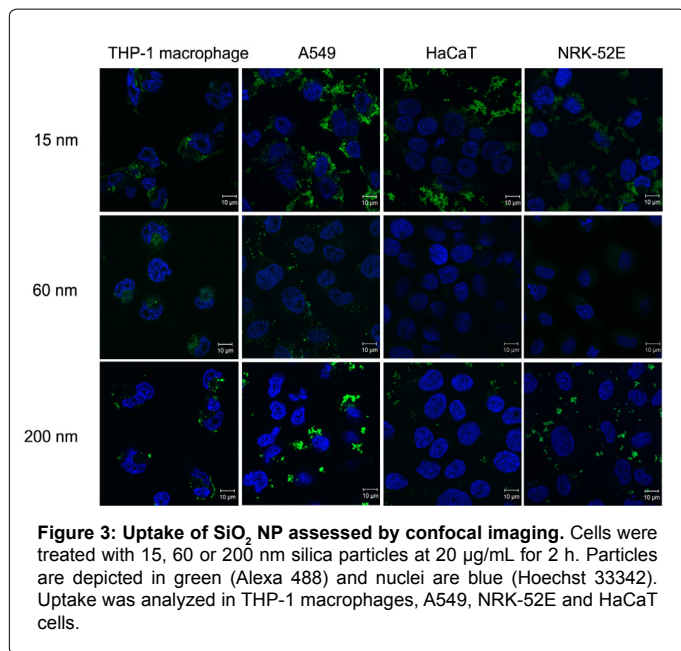
Thus, our data confirm a dose-dependent toxicity for 15 nm and 60 nm SiO₂ NP. If applied doses were compared on mass levels, we observed a clear size dependent effect, which vanished when applied doses were compared on the basis of the total NP surface area (Figure S3), indicating that the toxicity of SiO₂ NP is related to surface area.

Next we wanted to investigate whether the differences in toxicities were related to different uptake rates.

Different cell lines take up different amounts of SiO₂ NP

All cell lines were treated with 15, 60 and 200 nm SiO₂ NP at 20 µg/mL for 2 h and uptake was analyzed qualitatively with confocal microscopy (Figure 3). THP-1 macrophages rapidly took up 15 nm and 60 nm SiO₂ NP, already within 2 h. NP were present in small clusters, most likely representing vesicles. The nuclei were free of particles.

A549 also rapidly took up 15 nm and 60 nm particles, particles are



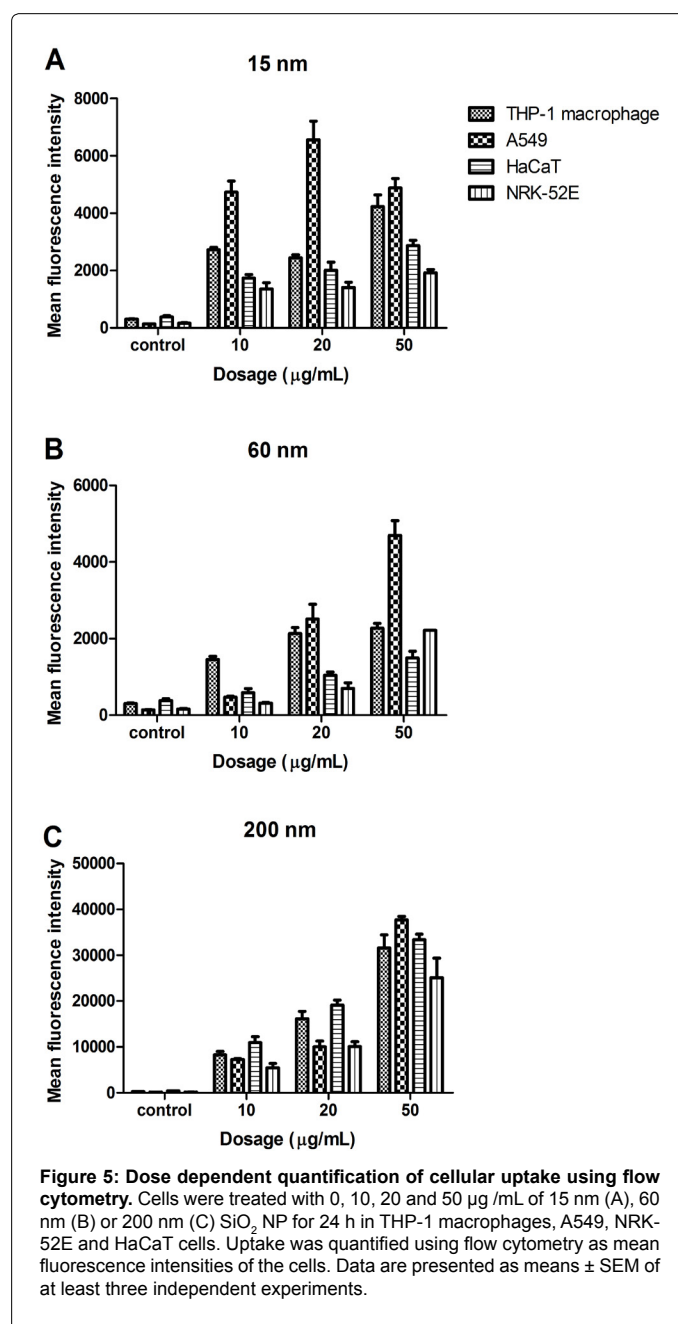
visible in clusters inside the cytoplasm already after 2 h. In contrast, NRK-52E cells rapidly took up only 15 nm but not 60 nm SiO₂ NP. In HaCaT cells 15 nm and 60 nm SiO₂ NP were localized clearly outside the cells after 2 h treatment (Figure 3), only after 24 h treatment SiO₂ NP was found inside cells (Figure S4). In all cell lines, the 200 nm particles hardly entered the cells after 2 h, but many of them attached to cell surface and were thus visible directly on the outer side of cell membrane. For all sizes of SiO₂ NP uptake was confirmed after 24 h treatment. In no case we found evidence that SiO₂ NP can be transported into the cell nuclei.

We then quantified uptake in all cell lines after 2h (Figure 4A) or 24h (Figure 4B) incubation using flow cytometry. For 60 nm and 200 nm SiO₂ NP the uptake profiles to all four cell lines were clearly time-dependent. However, the results for the 15 nm SiO₂ NP can be analyzed only after 24h as the analysis after 2 h is confounded from extracellularly attached NP. For the 15 nm SiO₂ NP we therefore only quantified the uptake after 24 h, where we confirmed by confocal microscopy that the NP were clearly inside the cells and not attached to cell surfaces any more. For further studies we decided to apply a quencher, which allowed us to quantify intracellular fluorescence only.

After 24 h incubation we observe a dose-dependent uptake in all four cell lines by flow cytometry (Figure 5). There is a clear dose dependent uptake visible for the 200 nm SiO₂ NP in all cell lines (Figure

5C). For 60 nm SiO₂ NP this dose dependent uptake was also observed for A549, HaCaT and NRK-52E cells (Figure 5B). However, in THP-1 macrophages 60 nm SiO₂ NP are already exerting a significant toxicity at 20 μg/mL. For the same reason dose-dependent cellular uptake analysis was confounded for 15 nm SiO₂ NP in THP-1 and A549 cells (Figure 5A).

Using flow cytometry, we again could confirm that indeed THP-1 macrophages and A549 are taking up higher amounts of NP compared to HaCaT and NRK-52E cells. Thus, the amounts taken up correlate very well with the results of the toxicity study (compare results in Figures 2 and 5). Surprisingly, for the 200 nm SiO₂ NP the differences in uptake between the various cell lines were not as high. This could be an indication that the uptake mechanism for 200 nm NP is be different compared to uptake mechanisms for 15 or 60 nm NP.



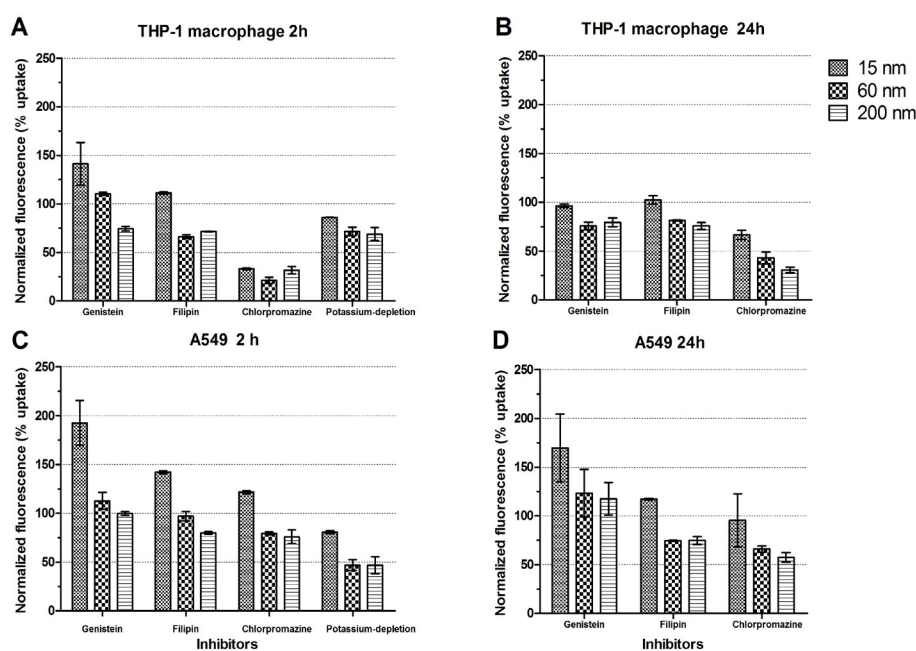


Figure 6: Analysis of uptake mechanisms using different inhibitors. Cells were pretreated with various inhibitors, Genistein, Filipin and Chlorpromazine, for 30 min, followed by exposure to SiO₂ NP in THP-1 macrophages (A and B) and A549 (C and D) cells for either 2 h (A and C) or 24 h (B and D). The uptake was quantified using flow cytometry as mean fluorescence intensities of the cells. Given are means ± SEM of 2 independent experiments, each with 3 replicas. The normalized fluorescence (% uptake) was calculated by dividing the SiO₂ NP fluorescence in the presence of inhibitor by the fluorescence of controls without inhibitors.

In the confocal images we have seen that the SiO₂ NP were not free in cytoplasm, but rather distinctly localized, most likely inside vesicles. We analyzed whether those vesicles represent lysosomes by using LysoTracker Red at different time points, 0.5, 2, 5 and 24 h after adding the NP. After 24 h we observed a significant co-localization between 15 nm SiO₂ NP and the lysosomal marker (Figure S5). This was not observed at earlier time points.

Size and cell type dependent uptake mechanisms for SiO₂ NP

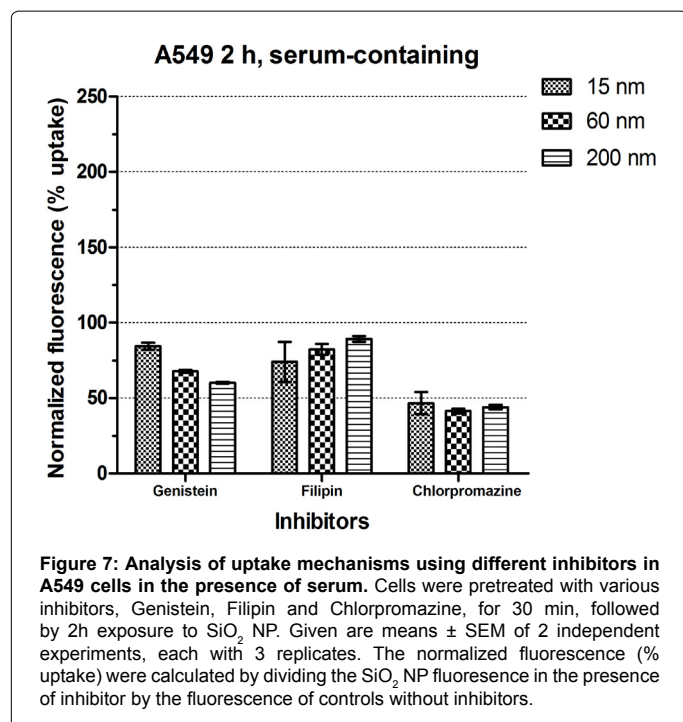
To further elucidate the uptake mechanisms we used specific inhibitors for clathrin-mediated and caveolin-mediated endocytosis. Genistein, which is a tyrosine kinase inhibitor, and filipin, which acts on cholesterol, were used as inhibitors to block the caveolin-mediated endocytosis. Chlorpromazine, a Rho GTPase inhibitor, and potassium-depletion, which is acting via clathrin removal, were used to inhibit the clathrin-mediated endocytosis. For that purpose we focused on THP-1 macrophages and A549 cells as they took up highest amounts of SiO₂ NP.

Prior to the experiment we carefully analyzed the cytotoxicity of the inhibitors after 2 and 24 h (Figures S6A-S6D) and used only sub-cytotoxic doses (cell viability higher than 80%). Potassium-depletion was only tolerated for 2 h. Furthermore we used fluorescent substrates to confirm the effect of the inhibitors at the applied doses. For that purpose we used BODIPY-LacCer as a substrate for caveolin-mediated endocytosis and transferrin-fluorescein for clathrin-mediated endocytosis. We analyzed the preferential uptake of transferrin by clathrin- and LacCer by caveolin-mediated endocytosis via immunostaining (Figure S7) and by applying specific inhibitors for the endocytotic pathway (Figure S8). The caveolin-mediated endocytosis could be blocked by genistein and filipin after 2 and 24 h in THP-1 by 10- 20% and in A549 by 20-30%

(Figure S8A). In A549 cells genistein did only reduce the uptake after 2 h but not after 24 h treatment. The clathrin-mediated uptake was blocked by chlorpromazine in THP-1 macrophages by approx. 40% at 2 and 24 h. In A549 cells chlorpromazine did not have any effect (Figure S8B). In A549 cells we also analyzed the uptake of clathrin and LacCer in the presence of serum (Figure S8C). The efficiency of potassium-depletion on the uptake of transferrin-fluorescein was checked by confocal microscopy (Figure S9). With the 3D images, it is clear that potassium-depletion indeed significantly reduced the uptake of transferrin. After potassium-depletion transferrin-fluorescein is mainly attached to the cell membrane but was not taken up. Thus, we could confirm that indeed the inhibitors used here did suppress the respective pathways to a certain extent. A full blockage was not observed and was also not expected.

In THP-1 macrophages caveolin specific inhibitors had no effect on the uptake of 15 nm SiO₂ NP. Filipin could decrease the uptake of the 60 and 200 nm SiO₂ after 2h and 24h (Figures 6A and 6B). In contrast, clathrin specific inhibitors could decrease the uptake for all three sizes of SiO₂ NP. After having applied chlorpromazine for 24h the uptake was decreased by 70% for the 200 nm particles, by 58% for 60 nm SiO₂ NP and only by 33% for 15 nm SiO₂ NP (Figure 6B). The uptake mechanism seems to be dependent on NP size.

In A549 cells the effects of the inhibitors were slightly different (Figures 6C and 6D). For the 15 nm SiO₂ the results were comparable to THP-1 macrophages. The inhibitors of the caveolin-mediated endocytosis had no effect on the uptake of the 15 nm NP but the potassium depletion could reduce the uptake by 19%. For 60 nm SiO₂ NP the inhibitors of the caveolin-mediated pathway had no effect in A549 cells after 2 h, which is in clear contrast to the results in THP-1 macrophages. However, after 24 h filipin could inhibit the uptake of



the 60 nm in A549 cells by 26%, which is similar to the result in THP-1 macrophages. Like in THP-1 cells, all inhibitors could block the uptake of the 200 nm particles.

These results indicate that the uptake mechanisms seem to be dependent in the cell type.

Finally, we investigated the uptake mechanisms also in the presence of serum in A549 cells (Figure 7). Firstly we observed differences in the total amount, which is taken up. At the same dosage (10 µg/mL), much less SiO₂ NP could be internalized into A549 cells in the presence of serum compared to serum free conditions (data not shown). In order to analyze the effects of the various inhibitors we had to increase the applied doses under serum containing conditions for all sizes to 100 µg/mL. However, no significant cytotoxicity was observed in serum-containing medium for all applied doses (Figure S10). The results revealed that for all particles all used inhibitors, i.e. genistein, filipin and chlorpromazine, could inhibit the uptake significantly. The caveolin specific inhibitors reduced the uptake by 20-40% while the clathrin specific chlorpromazine reduced the uptake by more than 50%. In addition we did not observe size-dependent differences in serum containing medium. However, when interpreting these results one needs to consider that in serum containing medium the SiO₂ NP (in particular the 15 or 60 nm NP) are significantly agglomerated such that final agglomerate sizes are very comparable for all three primary particle sizes. As the 200 nm SiO₂ NP are hardly agglomerated we focused our comparison of serum containing vs. serum free medium on the 200 nm SiO₂ NP. In serum containing medium, the treatment with chlorpromazine blocked the uptake of the 200 nm SiO₂ NP drastically. In serum-free medium in A549 cells in contrast all three inhibitors had a rather similar effect. This indicates that the uptake of the 200 nm particles in the presence of serum seems to be more specific, predominantly via the clathrin-mediated pathway.

Discussion

The cytotoxic effects of SiO₂ NP (15, 60, 200 nm) were investigated

in four different cell lines, A549, HaCaT, THP-1 derived macrophages and NRK-52E, which are representing different possible target organs (lung, skin, immune system and kidney). Most prominent effects were observed after exposure to 15 nm SiO₂ NP. The 60 nm SiO₂ NP caused less pronounced cytotoxicity and the 200 nm particles were not toxic at all. If applied doses are compared on mass levels, we observed a clear size dependent toxicity as also described by others [23,54,55]. Cytotoxicity, in particular for small SiO₂ NP, has been described already in various cell types, including lung cancer cells, myocardial cells or human endothelial cells [55-57]. Smaller NP have a larger specific surface (ie ratio of surface area to volume) leading to a higher surface reactivity [7,58,59]. It has been published that silica surfaces can generate ·OH radical, which may then cause cellular damage [31,60]. This may explain the higher toxicity observed for the small SiO₂ NP. Furthermore, for the 15 and 60 nm SiO₂ NP we detected a dose-dependent cytotoxicity as also observed by others [56,57].

Toxicity furthermore was dependent on the cell line. THP-1 macrophages were the most sensitive cell line followed by A549 cells. In contrast, HaCaT cells were rather tolerant. This may be explained by different physiological functions and correlated well to differences in uptake. Kroll et al. studied 23 NP in ten different cell lines [61] and also reported differences in the sensitivity of the cell lines. However, SiO₂ NP were not included in that study. Other studies using SiO₂ NP already found that epithelial cells or tumor cells were less sensitive compared to phagocytic cells or fibroblasts [62-64].

Interestingly the particle surface seems to be critical for explaining the toxicity of SiO₂ NP. Here we could confirm that differences in toxicity are vanishing after re-calculating the applied doses on the basis of NP surfaces [65].

Differences in toxicity may also be related to differences in NP uptake, which can be size dependent as well [42,43]. Via confocal microscopy and flow cytometry we could confirm that indeed the uptake of our NP was size and also cell-type dependent. Different uptake rates correlated very well with different toxicities. For instance, THP-1 macrophages and A549, which show the strongest toxicity, are taking up higher amounts of SiO₂ NP compared to HaCaT and NRK-52E cells. The 200 nm SiO₂ NP, which were non-toxic, hardly entered the cells within 2h. Thus, the SiO₂ uptake was not only dependent on NP size but also on the cell line. In another study, Nabeshi et al. also could correlate uptake and toxicity for different amorphous silica NP in Langerhans cells [54]. However, this study assessed only one cell type while in our study four different cell lines were compared.

In our study SiO₂ NP were taken up into the cytoplasm. We did not detect any SiO₂ NP in the cell nuclei. The majority of other studies also confirm that SiO₂ NP do not enter the cell nuclei, also for A549 cells [28,66,67]. Very rarely it has been published that SiO₂ NP can enter the nucleus. Zhu et al. report nuclear localization for 50 nm SiO₂ in HeLa cells [43]. Eventually, this may be related to different surface modifications of the silica [30].

The confocal images in our study confirm that the SiO₂ NP were rather distinctly localized in structures, most likely vesicles, in the cytosol. We could demonstrate that at least a part of them are lysosomes. Co-localization between SiO₂ NP and lysosomes could not be observed at early time points, only after 24h, suggesting that NP are taken up into endocytotic compartments, which are then trafficked and only later fused with lysosomal compartments [68]. Similar kinetics were reported by others. Rawi et al. investigated the uptake and intracellular localization of submicron and nano-sized SiO₂ particles in HeLa cells

and proved that SiO₂ NP (70 nm) are co-localized with lysosomes after 24 h. However, larger particles, ie 200 nm and 500 nm, show less lysosomal localization [69]. A possible explanation for this size-dependent localization of NP in lysosomes could be a size-dependent preference for clathrin versus caveolin mediated endocytosis [70].

Clathrin-mediated endocytosis (CME) is a receptor-mediated endocytosis and is involved in uptake of many nutrients such as LDL or iron-carrying transferrin. Specific receptors identify substrate and cargo them into “clathrin coated pits”, forming 60-200 nm vesicles that later enter the endosomal pathway and fuse with lysosomes [70]. Caveolae are a subtype of lift rafts and typically cluster in cholesterol-rich regions of plasma membrane, forming flask-shaped invaginations of 50-100 nm [71]. They are highly abundant in endothelial cells. In contrast to clathrin-coated pits caveolin remains attached to the vesicles and at least some of the vesicles seem to escape the fusion with lysosomes [72]. In general, the caveolin-mediated endocytosis is favored for nanomedicine because NP can escape lysosomal degradation via this pathway.

Here we used Chlorpromazine and a potassium-depleted buffer, two well-known inhibitors to block the clathrin-mediated pathway. Genistein and filipin were used to block the caveolin-mediated pathway. However, sometimes these inhibitors are not as selective and may as well block other uptake pathways [71]. We analyzed the efficiency of these inhibitors in our cell systems by using transferrin and lactosylceramide (LacCer) as substrates [70]. Chlorpromazine could strongly inhibit the uptake of transferrin in THP-1 macrophages but not in A549 cells, which is in contrast to results from another study, where it could block clathrin-mediated endocytosis in A549 cells by 90% [73]. Here, the effects of chlorpromazine appear to be cell type dependent. However, potassium-depletion worked very well for both cell types. By inhibiting clathrin-mediated endocytosis we could show that this pathway is involved in the uptake of all sizes of SiO₂ NP in both cell lines. In literature there is evidence that a broad size range of SiO₂ particles (50 nm - 600 nm) can be taken up by clathrin-mediated endocytosis in different cell types [17,27,40,43]. The caveolin-mediated pathway seems to contribute only for the 60 and 200 nm SiO₂ NP. Clearly it was not involved in uptake of the 15 nm NP. In contrast, inhibitors against the clathrin endocytosis had a stronger effect on the uptake of the 60 and 200 nm particles compared to inhibitors of the caveolin endocytosis. This suggests that for 60 and 200 nm SiO₂ NP the clathrin-mediated endocytosis is the main uptake route, although a part of the NP may enter the cells via the caveolin pathway. However, for 15 nm SiO₂ NP other uptake mechanisms should exist, which may be clathrin- and caveolin- independent.

So far uptake of SiO₂ NP smaller than 50 nm hardly has been analyzed. In one study 10 nm SiO₂ NP were shown to be taken up via both, clathrin and caveolin-mediated endocytosis in ovarian cancer cells [74]. Another study analyzed Sicastar Red-SiO₂ NP (30, 70 and 300 nm) in NCI-H441 and ISO-HAS-1 cells and found a clathrin- and caveolin-independent uptake mechanism [25,41]. The extent of SiO₂ uptake via clathrin-mediated pathway seems to change with size. Chlorpromazine was more effective in inhibiting the uptake of 200 nm polystyrene NP compared to 40 nm in A549 cells [73]. We observe similar results. Also in our study chlorpromazine was more effective towards 60 and 200 nm SiO₂.

We also observed differences in the uptake of the 60 nm SiO₂ between A549 cells and THP-1 macrophages. For the uptake of polystyrene NP cell-type dependent differences in uptake mechanisms

already have been described for HeLa, A549 and 1321N1 cells [73]. Similar studies with SiO₂ NP are not published.

It is well known that NP in biological fluids are covered by a so-called “protein corona”. We also detect protein adsorption to our SiO₂ NP, which in turn caused massive agglomeration in serum containing media, especially for the 15 and 60 nm SiO₂. Moreover, in serum containing medium the uptake of SiO₂ NP is drastically reduced, which was also detected in other studies [45,46]. In these studies it has been observed that in the presence of serum SiO₂ NP show a reduced adhesion to the cell membrane, leading to a reduced cellular uptake. This has been confirmed here. Concerning the uptake mechanisms we focused our comparison between serum containing and serum-free conditions on the 200 nm SiO₂ as the 15 and 60 nm SiO₂ were strongly agglomerated in the presence of serum. Our data indicate that the uptake mechanisms for 200 nm SiO₂ seem to be more specific in the presence of serum. The inhibitor, in particular chlorpromazine, had a much stronger inhibitory effect in the presence of serum. The 200 nm SiO₂ NP seem to be nearly exclusively taken up by the clathrin pathway under serum containing conditions. Eventually the presence of proteins on the surface of the NP is supporting the receptor-mediated recognition.

Furthermore it should be noted that also the cytotoxicity is changing significantly in the presence of serum as in the presence of serum no toxicity is observed. Eventually in the absence of serum SiO₂ NP may also penetrate the cells directly without prior interaction to specific receptors as they are highly protein adsorptive. This may cause cell death. It would be highly interesting to compare also the uptake mechanisms for smaller sizes of SiO₂ NP in the presence and absence of serum. For that purpose one would require SiO₂ NP that do not agglomerate in the presence of serum.

In summary, our data confirm that the uptake mechanisms for SiO₂ NP are strongly dependent on the NP sizes but also on the cell lines used in the study. In particular for the smaller particles (15 nm diameter) we find evidence that also other pathways being independent of clathrin and caveolin strongly contribute to the uptake, at least under serum free conditions. Clathrin mediated endocytosis seems to contribute to the uptake of all sizes used in this study while caveolin mediated endocytosis plays only a minor role and is involved only for the uptake of 60 and 200 nm SiO₂ NP. In future studies it might be interesting to design special types of SiO₂ NP by using different surface coatings, which are stable in the presence of serum and which are taken up more specifically via caveolin-mediated endocytosis, which may be superior for medical applications.

Conclusion

Here we analyse the uptake and the uptake mechanisms of SiO₂ NP using a well-suited fluorescently labeled core-shell SiO₂ NP system to prevent dye-leakage and alteration of the NP surface properties via dye attachment. The fluorescently labeled core-shell SiO₂ NP have been specifically synthesized for the purpose of this study. We use three different sizes (i.e 15, 60 and 200 nm) and four different cell lines representing different uptake routes or important secondary target organs, i.e a lung related cell line (A549), a skin related cell line (HaCaT), kidney cells (NRK-52E) and macrophage like cells (THP-1 derived). We observe a size dependent cytotoxicity in all four cell lines in serum free conditions, which correlated well with different uptake into the four cell types. Clathrin-mediated endocytosis was involved in uptake of all sizes of SiO₂ particles in THP-1 macrophages and in A549 cells. Caveolin-mediated endocytosis contributed to the uptake of 60 and 200 nm SiO₂ NP in THP-1 macrophages but only to uptake of 200

nm SiO₂ NP in A549. Interestingly for the 15 nm SiO₂ the caveolin-mediated endocytosis seems not be involved. Thus, we find evidence that another pathway, which is clathrin- and caveolin- independent, could be involved in the uptake of the 15 nm SiO₂ NP.

In the presence of serum, all sizes of SiO₂ NP become non toxic and the uptake in general is significantly reduced. Furthermore the uptake mechanisms may change. For the 200 nm SiO₂ NP the uptake seems to be more specific, now mostly exclusively via the clathrin-mediated endocytosis.

In summary, this study demonstrates size- and cell type dependent differences in SiO₂ NP uptake and in uptake mechanisms, which could be relevant for potential use of SiO₂ NP as a drug delivery system in the medical field.

Acknowledgement

The authors acknowledge funding from BfR and TU. I-Lun Hsiao also thanks DAAD and the Ministry of Science and Technology Taiwan (MOST) for financial support.

References

1. Project on Emerging Nanotechnologies. Nanotechnology consumer products inventory analysis ; updated 2013 October. Accessed May 20, 2014.
2. Hansen SF, Michelson ES, Kamper A, Borling P, Stuer-Lauridsen F, et al. (2008) Categorization framework to aid exposure assessment of nanomaterials in consumer products. *Ecotoxicology* 17: 438-447.
3. Athinarayanan J, Periasamy VS, Alsaif MA, Al-Warthan AA, Alshatwi AA (2014) Presence of nanosilica (E551) in commercial food products: TNF-mediated oxidative stress and altered cell cycle progression in human lung fibroblast cells. *Cell Biol Toxicol* 30: 89-100.
4. Biju V (2014) Chemical modifications and bioconjugate reactions of nanomaterials for sensing, imaging, drug delivery and therapy. *Chem Soc Rev* 43: 744-764.
5. Yang PP, Gai SL, Lin J (2012) Functionalized mesoporous silica materials for controlled drug delivery. *Chem Soc Rev* 41: 3679-3698.
6. Tallury P, Payton K, Santra S (2008) Silica-based multimodal/multifunctional nanoparticles for bioimaging and biosensing applications. *Nanomedicine* 3: 579-592.
7. Oberdorster G, Oberdorster E, Oberdorster J (2005) Nanotoxicology: An emerging discipline evolving from studies of ultrafine particles. *Environ Health Perspect* 113: 823-839.
8. Landsiedel R, Ma-Hock L, Hofmann T, Wiemann M, Strauss V, et al. (2014) Application of short-term inhalation studies to assess the inhalation toxicity of nanomaterials. *Part Fibre Toxicol* 11:16.
9. Arts JH, Muijsers H, Duistermaat E, Junker K, Kuper CF (2007) Five-day inhalation toxicity study of three types of synthetic amorphous silicas in Wistar rats and post-exposure evaluations for up to 3 months. *Food Chem Toxicol* 45: 1856-1867.
10. Park EJ, Roh J, Kim Y, Choi K (2011) A single instillation of amorphous silica nanoparticles induced inflammatory responses and tissue damage until Day 28 after exposure. *J Health Sci* 57: 60-71.
11. Hirai T, Yoshikawa T, Nabeshi H, Yoshida T, Akase T, et al. (2012) Dermal absorption of amorphous nanosilica particles after topical exposure for three days. *Pharmazie* 67: 742-743.
12. Rancan F, Gao Q, Graf C, Troppens S, Hadam S, et al. (2012) Skin penetration and cellular uptake of amorphous silica nanoparticles with variable size, surface functionalization, and colloidal stability. *ACS Nano* 6: 6829-6842.
13. van der Zande M, Vandebriel RJ, Groot MJ, Kramer E, Herrera Rivera ZE, et al. (2014) Sub-chronic toxicity study in rats orally exposed to nanostructured silica. *Part Fibre Toxicol* 11:8.
14. Sakai N, Takakura M, Imamura H, Sugimoto M, Matsui Y, et al. (2012) Whole-body distribution of C-14-labeled silica nanoparticles and submicron particles after intravenous injection into Mice. *J Nanopart Res* 14: 849.
15. Yu Y, Li Y, Wang W, Jin M, Du Z, et al. (2013) Acute toxicity of amorphous silica nanoparticles in intravenously exposed ICR mice. *PLoS One* 8: e61346.
16. Lu X, Qian JC, Zhou HJ, Gan Q, Tang W, et al. (2011) In vitro cytotoxicity and induction of apoptosis by silica nanoparticles in human HepG2 hepatoma cells. *Int J Nanomed* 6: 1889-1901.
17. Passagne I, Morille M, Rousset M, Pujalte I, L'Azou B (2012) Implication of oxidative stress in size-dependent toxicity of silica nanoparticles in kidney cells. *Toxicology* 299: 112-124.
18. Skuland T, Ovrevik J, Lag M, Refsnes M (2014) Role of size and surface area for pro-inflammatory responses to silica nanoparticles in epithelial lung cells: Importance of exposure conditions. *Toxicol Vitro* 28: 146-155.
19. Park M, Lynch I, Ramirez-Garcia S, Dawson KA, de la Fonteyneet L, et al. (2011) In vitro evaluation of cytotoxic and inflammatory properties of silica nanoparticles of different sizes in murine RAW 264.7 macrophages. *J Nanopart Res* 13: 6775-6787.
20. Duan JC, Yu YB, Li Y, Yu Y, Li Y, et al. (2013) Toxic effect of silica nanoparticles on endothelial cells through DNA damage response via Chk1-dependent G2/M checkpoint. *PLoS One* 8: e62087.
21. Ahmad J, Ahamed M, Akhtar MJ, Alokayan SA, Siddiqui MA, et al. (2012) Apoptosis induction by silica nanoparticles mediated through reactive oxygen species in human liver cell line HepG2. *Toxicol Appl Pharmacol* 259: 160-168.
22. Mohamed BM, Verma NK, Prina-Mello A, Williams Y, Davies AM, et al. (2011) Activation of stress-related signalling pathway in human cells upon SiO₂ nanoparticles exposure as an early indicator of cytotoxicity. *J Nanobiotechnol* 9: 29.
23. Li Y, Sun L, Jin MH, Du Z, Liu X, et al. (2011) Size-dependent cytotoxicity of amorphous silica nanoparticles in human hepatoma HepG2 cells. *Toxicol Vitro* 25: 1343-1352.
24. Liang H, Jin C, Tang Y, Wang F, Ma C, et al. (2014) Cytotoxicity of silica nanoparticles on HaCaT cells. *J Appl Toxicol* 34: 367-372.
25. Kasper J, Hermanns MI, Bantz C, Koshkina O, Lang T, et al. (2013) Interactions of silica nanoparticles with lung epithelial cells and the association to flotillins. *Arch Toxicol* 87: 1053-1065.
26. McCarthy J, Inkielewicz-Stepniak I, Corbalan JJ, Radomski MW (2012) Mechanisms of toxicity of amorphous silica nanoparticles on human lung submucosal cells in vitro: protective effects of Fisetin. *Chem Res Toxicol* 25: 2227-2235.
27. Blechinger J, Bauer AT, Torrano AA, Gorzelanny C, Bräuchle C, et al. (2013) Uptake kinetics and nanotoxicity of silica nanoparticles are cell type dependent. *Small* 9: 3970-3980.
28. Mu QS, Hondow NS, Krzeminski L, Brown AP, Jeuken LJ, et al. (2012) Mechanism of cellular uptake of genotoxic silica nanoparticles. *Part Fibre Toxicol* 9: 29.
29. Yu T, Malugin A, Ghandehari H (2011) Impact of silica nanoparticle design on cellular toxicity and hemolytic activity. *ACS Nano* 5: 5717-5728.
30. Nabeshi H, Yoshikawa T, Arimori A, Yoshida T, Tochigi S, et al. (2011) Effect of surface properties of silica nanoparticles on their cytotoxicity and cellular distribution in murine macrophages. *Nanoscale Res Lett* 6: 93.
31. Napierska D, Thomassen LCJ, Lison D, Martens JA, Hoet PH (2010) The nanosilica hazard: another variable entity. *Part Fibre Toxicol* 7: 39.
32. Marzaioli V, Aguilar-Pimentel JA, Weichenmeier I, Luxenhofer G, Wiemann M, et al. (2014) Surface modifications of silica nanoparticles are crucial for their inert versus proinflammatory and immunomodulatory properties. *Int J Nanomed* 9: 2815-2832.
33. Sayes CM, Reed KL, Warheit DB (2007) Assessing toxicity of fine and nanoparticles: Comparing in vitro measurements to in vivo pulmonary toxicity profiles. *Toxicol Sci* 97: 163-180.
34. Lee S, Kim MS, Lee D, Kwon TK, Khang D, et al. (2013) The comparative immunotoxicity of mesoporous silica nanoparticles and colloidal silica nanoparticles in mice. *Int J Nanomed* 8: 147-158.
35. Kennedy IM, Wilson D, Barakat AI (2009) Uptake and inflammatory effects of nanoparticles in a human vascular endothelial cell line. *Res Rep Health Eff Inst* 136: 3-32.
36. Wang JD, Teng ZG, Tian Y, Fang T, Ma J, et al. (2013) Increasing cellular uptake of mesoporous silica nanoparticles in human embryonic kidney cell line 293T cells by using Lipofectamine 2000. *J Biomed Nanotechnol* 9: 1882-1890.

37. Lu F, Wu SH, Hung Y, Mou CY (2009) Size effect on cell uptake in well-suspended, uniform mesoporous silica nanoparticles. *Small* 5: 1408-1413.
38. Gliga AR, Skoglund S, Wallinder IO, Fadeel B, Karlsson HL (2014) Size-dependent cytotoxicity of silver nanoparticles in human lung cells: the role of cellular uptake, agglomeration and Ag release. *Part Fibre Toxicol* 11: 11.
39. dos Santos T, Varela J, Lynch I, Salvati A, Dawson KA (2011) Quantitative assessment of the comparative nanoparticle-uptake efficiency of a range of cell lines. *Small* 7: 3341-3349.
40. Hu L, Mao Z, Zhang Y, Gao C (2011) Influences of size of silica particles on the cellular endocytosis, exocytosis and cell activity of HepG2 cells. *J Nanoscience Lett* 1: 1-16.
41. Kasper J, Hermanns MI, Bantz C, Utech S, Koshkina O, et al. (2013) Flotillin-involved uptake, of silica nanoparticles and responses of an alveolar-capillary barrier in vitro. *Eur J Pharm Biopharm* 84: 275-287.
42. Shapero K, Fenaroli F, Lynch I, Cottell DC, Salvati A, et al. (2011) Time and space resolved uptake study of silica nanoparticles by human cells. *Mol Biosyst* 7: 371-378.
43. Zhu J, Liao L, Zhu LN, Zhang P, Guo K, et al. (2013) Size-dependent cellular uptake efficiency, mechanism, and cytotoxicity of silica nanoparticles toward HeLa cells. *Talanta* 107: 408-415.
44. Vranic S, Boggetto N, Contremoulins V, Mornet S, Reinhardt N, et al. (2013) Deciphering the mechanisms of cellular uptake of engineered nanoparticles by accurate evaluation of internalization using imaging flow cytometry. *Part Fibre Toxicol* 10: 2.
45. Lesniak A, Fenaroli F, Monopoli MR, Åberg C, Dawson KA, et al. (2012) Effects of the presence or absence of a protein corona on silica nanoparticle uptake and impact on cells. *ACS Nano* 6: 5845-5857.
46. Lesniak A, Salvati A, Santos-Martinez MJ, Radomski MW, Dawson KA, et al. (2013) Nanoparticle adhesion to the cell membrane and its effect on nanoparticle uptake efficiency. *J Am Chem Soc* 135: 1438-1444.
47. Kendall M, Ding P, Kendall K (2011) Particle and nanoparticle interactions with fibrinogen: the importance of aggregation in nanotoxicology. *Nanotoxicology* 5: 55-65.
48. Turci F, Ghibaudo E, Colonna M, Boscolo B, Fenoglio I, et al. (2010) An integrated approach to the study of the interaction between proteins and nanoparticles. *Langmuir* 26: 8336-8346.
49. Yan Y, Gause KT, Kamphuis MM, Ang CS, O'Brien-Simpson NM, et al. (2013) Differential roles of the protein corona in the cellular uptake of nanoporous polymer particles by monocyte and macrophage cell lines. *ACS Nano* 7: 10960-10970.
50. Lunov O, Syrovets T, Loos C, Beil J, Delacher M, et al. (2012) Differential uptake of functionalized polystyrene nanoparticles by human macrophages and monocytic cells. *ACS Nano* 5: 1657-1669.
51. Salvati A, Åberg C, dos Santos T, Varela J, Pinto P, et al. (2011) Experimental and theoretical comparison of intracellular import of polymeric nanoparticles and small molecules: toward models of uptake kinetics. *Nanomed-Nanotechnol Biol Med* 7: 818-826.
52. Joksimovic R, Altin B, Mehta SK, Gradzielski M (2013) Synthesis of silica nanoparticles covered with silver beads. *J Nanosci Nanotechnol* 13: 6773-6781.
53. Kahlert S, Zundorf G, Reiser G (2005) Glutamate-mediated influx of extracellular Ca^{2+} is coupled with reactive oxygen species generation in cultured hippocampal neurons but not in astrocytes. *J Neurosci Res* 79: 262-271.
54. Nabeshi H, Yoshikawa T, Matsuyama K, Nakazato Y, Arimori A, et al. (2010) Size-dependent cytotoxic effects of amorphous silica nanoparticles on Langerhans cells. *Pharmazie* 65: 199-201.
55. Napierska D, Thomassen LCJ, Rabolli V, Lison D, Gonzalez L, et al. (2009) Size-dependent cytotoxicity of monodisperse silica nanoparticles in human endothelial cells. *Small* 5: 846-853.
56. Lin WS, Huang YW, Zhou XD, Ma YF (2006) In vitro toxicity of silica nanoparticles in human lung cancer cells. *Toxicol Appl Pharmacol* 217: 252-259.
57. Ye YY, Liu JW, Chen MC, Sun LJ, Lan MB (2010) In vitro toxicity of silica nanoparticles in myocardial cells. *Environ Toxicol Pharmacol* 29: 131-137.
58. Nel A, Xia T, Madler L, Li N (2006) Toxic potential of materials at the nanolevel. *Science* 311: 622-627.
59. Kipen HM, Laskin DL (2005) Smaller is not always better: nanotechnology yields nanotoxicology. *Am J Physiol-Lung Cell Mol Physiol*. 289: L696-L697.
60. Shang Y, Zhu T, Li Y, Zhao J (2009) Size-dependent hydroxyl radicals generation induced by SiO_2 ultra-fine particles: The role of surface iron. *Sci China Ser B*. 52: 1033-1041.
61. Kroll A, Dierker C, Rommel C, Hahn D, Wohlleben W, et al. (2011) Cytotoxicity screening of 23 engineered nanomaterials using a test matrix of ten cell lines and three different assays. *Part Fibre Toxicol* 8: 9.
62. Chang JS, Chang KLB, Hwang DF, Kong ZL (2007) In vitro cytotoxicity of silica nanoparticles at high concentrations strongly depends on the metabolic activity type of the cell line. *Environ Sci Technol* 41: 2064-2068.
63. Lanone S, Rogerieux F, Geys J, Dupont A, Maillot-Marechal E, et al. (2009) Comparative toxicity of 24 manufactured nanoparticles in human alveolar epithelial and macrophage cell lines. *Part Fibre Toxicol* 6: 14.
64. Hamilton RF, Thakur SA, Holian A (2008) Silica binding and toxicity in alveolar macrophages. *Free Radic Biol Med* 44: 1246-1258.
65. Guthrie GD, Heaney PJ (1995) Mineralogical characteristics of silica polymorphs in relation to their biological activities. *Scand J Work Environ Health* 21: 5-8.
66. Jin YH, Kannan S, Wu M, Zhao JX (2007) Toxicity of luminescent silica nanoparticles to living cells. *Chem Res Toxicol* 20: 1126-1133.
67. Stayton I, Winiarz J, Shannon K, Ma YF (2009) Study of uptake and loss of silica nanoparticles in living human lung epithelial cells at single cell level. *Anal Bioanal Chem* 394: 1595-1608.
68. Huang DM, Hung Y, Ko BS, Hsu SC, Chen WH, et al. (2005) Highly efficient cellular labeling of mesoporous nanoparticles in human mesenchymal stem cells: implication for stem cell tracking. *Faseb J* 19: 2014-2016.
69. Al-Rawi M, Diabate S, Weiss C (2011) Uptake and intracellular localization of submicron and nano-sized SiO_2 particles in HeLa cells. *Arch Toxicol* 85: 813-826.
70. Rejman J, Oberle V, Zuhorn IS, Hoekstra D (2004) Size-dependent internalization of particles via the pathways of clathrin- and caveolae-mediated endocytosis. *Biochem J* 377: 159-169.
71. Sahay G, Alakhova DY, Kabanov AV (2010) Endocytosis of nanomedicines. *J Control Release* 145: 182-195.
72. Kiss AL, Botos E (2009) Endocytosis via caveolae: alternative pathway with distinct cellular compartments to avoid lysosomal degradation? *J Cell Mol Med* 13: 1228-1237.
73. dos Santos T, Varela J, Lynch I, Salvati A, Dawson KA (2011) Effects of transport inhibitors on the cellular uptake of carboxylated polystyrene nanoparticles in different cell lines. *PLoS One* 6: e24438.
74. Ekkapongpisit M, Giovia A, Follo C, Caputo G, Isidoro C (2012) Biocompatibility, endocytosis, and intracellular trafficking of mesoporous silica and polystyrene nanoparticles in ovarian cancer cells: effects of size and surface charge groups. *Int J Nanomed* 7: 4147-4158.